Infrared Spectra and Structures of the $OSc(N_2)$, OScNN, and $OScNN^+$ Complexes in Solid Argon

Mingfei Zhou,* Guanjun Wang, Yanying Zhao, Mohua Chen, and Chuanfan Ding

Department of Chemistry & Laser Chemistry Institute, Shanghai Key Laboratory of Molecular Catalysts and Innovative Materials, Fudan University, Shanghai 200433, P. R. China

Received: February 24, 2005; In Final Form: April 26, 2005

Scandium monoxide−dinitrogen complexes—$OSc(N_2)$, OScNN, and $OScNN^+$—have been prepared by the reactions of laser-evaporated scandium monoxide with N_2 or scandium atoms with N_2O in solid argon. The ground-state scandium monoxide molecule reacted with N_2 to form the side-bonded $OSc(N_2)$ complex spontaneously on annealing. This complex rearranged to the end-on bonded OScNN complex upon UV irradiation. Both the $OSc(N_2)$ and OScNN complexes in solid argon can be assigned to have $^2A''$ electronic ground state with C_s symmetry arising from the $^2\Delta$ first excited-state ScO. The neutral complexes can also be photoionized to the $OScNN^+$ cation complex upon UV irradiation.

Introduction

Coordination of dinitrogen to transition metal centers is proposed to be the initial step of the complex sequential chemical activation of dinitrogen. Dinitrogen binding to the transition metal center weakens the N−N bond and makes it potentially activatable. A number of experimental and theoretical studies have been carried out to examine the interactions of transition metal atoms and cations with dinitrogen,[1−9] and hundreds of transition metal−dinitrogen complexes with different coordination modes have been characterized.[10−12]

Transition metal oxides are widely used as catalysts and catalytic support. However, the reactions of transition metal oxide molecules with dinitrogen have received quite little attention. Scandium monoxide is the simplest transition metal oxide. It provides an ideal starting point for understanding the interactions of transition metal oxides with dinitrogen. Recent studies by Hwang and Mebel have demonstrated that scandium monoxide (ScO) enhanced the reaction of nitrogen hydrogenation.[13]

The matrix isolation technique has been developed to the study of a wide range of species, including free radicals, ions, and weakly bound complexes. Recent investigations in our laboratory on the reactions of transition metal atoms and compounds with dinitrogen molecules have characterized a number of transition metal−dinitrogen complexes in solid matrices.[14−16] In this paper, we report a combined matrix-isolation infrared absorption spectroscopic and density functional theoretical study of the scandium monoxide−dinitrogen complexes—$OSc(N_2)$, OScNN and $OScNN^+$—generated by the reactions of laser-evaporated scandium monoxide with N_2 or scandium atoms with N_2O in solid argon.

Experimental and Computational Methods

The experimental setup for pulsed laser evaporation and matrix isolation infrared spectroscopic investigation has been described previously.[17] Briefly, the 1064 nm Nd:YAG laser fundamental (Spectra Physics, DCR 150, 20 Hz repetition rate and 8 ns pulse width) was focused onto the rotating scandium metal or metal oxide (Sc_2O_3) target through a hole in a CsI window, which was mounted on a cold tip of a closed-cycle helium refrigerator (Air Products, model CSW202). The refrigerator was located in a vacuum shrouds, which was maintained at $(2-4) \times 10^{-4}$ Pa during experiments. Typically, 5−10 mJ/pulse laser energy was used. The ablated species were codeposited with N_2 or N_2O in excess argon onto the 12 K CsI window for one to 2 h at a rate of approximately 5 mmol/h. The N_2/Ar and N_2O/Ar mixtures were prepared in a stainless steel vacuum line using standard manometric technique. Isotopic substituted $^{15}N_2$ and $^{14}N_2 + {}^{15}N_2$ and $^{14}N_2 + {}^{14}N^{15}N + {}^{15}N_2$ mixtures were used in different experiments. Infrared spectra were recorded on a Bruker IFS113v spectrometer at 0.5 cm^{-1} resolution with a DTGS detector in the spectral range of 4000−400 cm^{-1}. Matrix samples were annealed at different temperatures, and selected samples were subjected to broadband irradiation at 12 K using a 250 W high-pressure mercury arc lamp and glass filters, and more spectra were taken.

Density functional calculations were performed using the Gaussian 03 program.[18] The most popular Becke's three-parameter hybrid functional, with additional correlation corrections due to Lee, Yang, and Parr was utilized (B3LYP).[19,20] The 6-311++G** basis set was used for N and O, and the all electron basis set of Wachters-Hay as modified by Gaussian was used for Sc.[21,22] The geometries were fully optimized; the harmonic vibrational frequencies were calculated with analytic second derivatives, and zero-point vibrational energies (ZPVE) were derived. Transition state optimizations were done with the synchronous transit-guided quasi-Newton (STQN) method. [23]

Results

$Sc_2O_3 + N_2$/Ar. Experiments were run using a Sc_2O_3 target. Codeposition of laser evaporated oxides with pure argon at 12 K forms ScO (954.8 cm^{-1} with a site absorption at 951.8 cm^{-1}) as the major product with minor ScO^+ (976.4 cm^{-1}) and ScO_2^- (722.5 cm^{-1}).[24,25] These absorptions show no obvious change on annealing. Broadband irradiation almost destroyed the ScO_2^- absorption, slightly increased the ScO^+ absorption at the expense of the ScO absorption. In addition, a weak band was observed

* Corresponding author. E-mail: mfzhou@fudan.edu.cn.

10.1021/jp050975b CCC: $30.25
Published on Web 05/21/2005

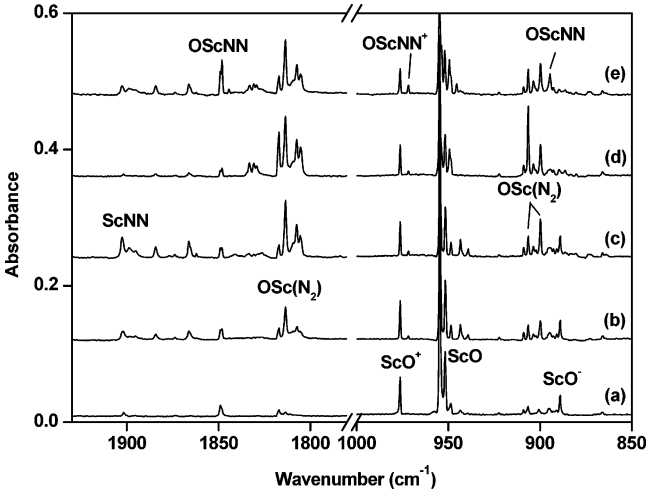

Figure 1. Infrared spectra in the 1930−1780 and 1000−850 cm^{-1} regions from codeposition of laser-evaporated ScO with 0.05% N_2 in argon at 12 K. (a) 2 h of sample deposition, (b) after 25 K annealing, (c) after 30 K annealing, (d) after 20 min of $\lambda > 500$ nm irradiation, and (e) after 20 min of $\lambda > 250$ nm irradiation.

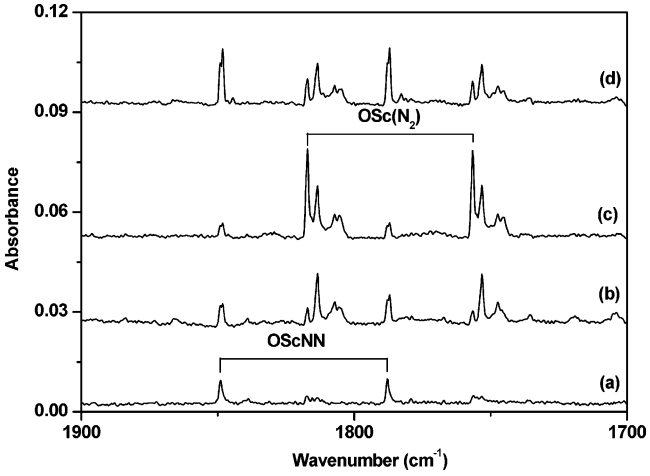

Figure 2. Infrared spectra in the 1900−1700 cm^{-1} region from codeposition of laser-evaporated ScO with 0.075% $^{14}N_2$ + 0.075% $^{15}N_2$ in argon at 12 K. (a) 2 h of sample deposition, (b) after 25 K annealing, (c) after 20 min of $\lambda > 500$ nm irradiation, and (d) after 20 min of $\lambda > 250$ nm irradiation.

at 889.2 cm^{-1}. This band slightly decreased on annealing, disappeared on broadband irradiation, and is assigned to the ScO^- anion. Previous photoelectron spectroscopic study in the gas phase yielded a vibrational frequency for the ScO^- anion to be 840 ± 60 cm^{-1}.[26] B3LYP calculations predicted that the ScO^- anion has a $^1\Sigma^+$ ground state with a Sc−O stretching frequency at 934.1 cm^{-1}, 65.7 cm^{-1} lower than that of ScO calculated at the same level. The experimentally observed difference between ScO and ScO^- in solid argon is 65.6 cm^{-1}.

New product absorptions were produced when different concentration N_2/Ar mixtures were used as the reagent gas. The spectra in the N−N stretching and Sc−O stretching frequency regions from codeposition of laser-evaporated scandium oxides with 0.05% N_2 in argon are shown in Figure 1, and the product absorptions are listed in Table 1. After sample deposition (trace a), weak features were observed at 1849.2, 1817.2, 1813.6, 906.5, 899.8, and 894.6 cm^{-1}. On the basis of their growth/decay characteristics measured as a function of changes of experimental conditions, these absorptions can be grouped into three pairs. The 1817.2/906.5 cm^{-1} pair slightly increased when the matrix was annealed to 25 (trace b) and 30 K (trace c), markedly enhanced when the matrix was irradiated by the output of the high-pressure mercury arc lamp with a $\lambda > 400$ nm pass filter ($400 < \lambda < 580$ nm, trace d), but decreased significantly upon continued irradiation without pass filter ($250 < \lambda < 580$ nm) (trace e). The 1813.6/899.8 cm^{-1} pair increased on sample annealing, but kept almost unchanged upon different wavelength range irradiation. The 1849.2/894.6 cm^{-1} pair is weak upon sample deposition and showed no obvious change upon sample annealing, but increased significantly upon $250 < \lambda < 580$ nm broadband irradiation. A weak new band at 971.8 cm^{-1} was produced on broadband irradiation as well. In addition, weak absorptions due to ScNN (1902.7 cm^{-1}),[27] HScOH,[28,29] HScOH(NN) (1884.3 and 1442.8 cm^{-1}), and $HScOH(N_2)$ (1832.9 and 1476.9 cm^{-1})[16] were also observed in the experiments.

The experiments were repeated using the isotopic labeled $^{15}N_2$, $^{14}N_2 + {}^{15}N_2$, and $^{14}N_2 + {}^{14}N^{15}N + {}^{15}N_2$ samples. The isotopic shifts and splittings are also listed in Table 1. Figure 2 shows the spectra in the N−N stretching frequency region using a 0.075% $^{14}N_2$ + 0.075% $^{15}N_2$ sample. The spectra in the in the 1880−1700 cm^{-1} region with a 0.05% $^{14}N_2$ + 0.1% $^{14}N^{15}N$ + 0.05% $^{15}N_2$ sample are illustrated in Figure 3.

Sc + N_2O/Ar. A supplemental experiment was conducted with a scandium metal target and 0.2% N_2O in argon. The resulting spectra in the N−N and Sc−O stretching frequency regions are shown in Figure 4. After deposition, product absorptions at 2341.7 (not shown), 1849.2, 1817.2, 971.8, 906.5, and 894.6 cm^{-1}, as well as ScO, ScO^+, and NNO_2^- (not shown)[30] absorptions, were seen in the spectrum (trace a). When this matrix was irradiated at the wavelength range of $400 < \lambda < 580$ nm (trace c), the 1817.2 and 906.5 cm^{-1} bands were greatly enhanced at the expense of the 1849.2 and 894.6 cm^{-1}

TABLE 1: Infrared Absorptions (cm^{-1}) from Codeposition of Laser-Evaporated Scandium Oxide with N_2 or Scandium Atoms with N_2O in Excess Argon

$^{14}N_2$	$^{15}N_2$	$^{14}N_2 + {}^{15}N_2$	$^{14}N_2 + {}^{14}N^{15}N + {}^{15}N_2$	assignment
2341.7				$OScNN^+$
1902.7	1840.5	1902.7, 1840.5		ScNN
1849.2	1788.0	1849.2, 1788.0	1849.2, 1819.3, 1817.8, 1788.0	OScNN
1848.3	1781.1	1848.3, 1781.1		OScNN site
1817.2	1756.6	1817.2, 1756.6	1817.2, 1787.0, 1756.6	$OSc(N_2)$
1813.6	1753.3	1813.6, 1753.3	1813.6, 1783.7, 1753.3	$OSc(N_2)(NN)_x$
1807.5	1747.4	1807.5, 1747.4	1807.5, 1777.9, 1747.4	$OSc(N_2)(NN)_x$
976.4	976.4			ScO^+
971.8	971.8			$OScNN^+$
954.8	954.8			ScO
951.8	951.8			ScO site
906.5	906.5			$OSc(N_2)$
899.8	899.8			$OSc(N_2)(NN)_x$
894.6	894.4			OScNN
889.2	889.2			ScO^-

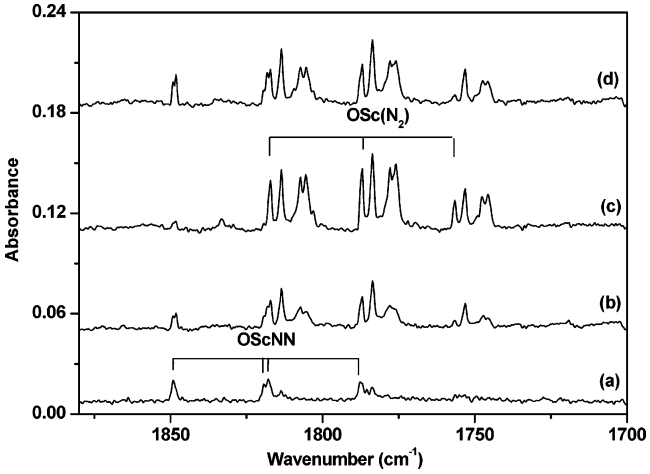

Figure 3. Infrared spectra in the 1880−1700 cm^{-1} region from codeposition of laser-evaporated ScO with 0.05% $^{14}N_2$ + 0.1% $^{14}N^{15}N$ + 0.05% $^{15}N_2$ in argon at 12 K. (a) 2 h of sample deposition, (b) after 25 K annealing, (c) after 20 min of $\lambda > 500$ nm irradiation, and (d) after 20 min of $\lambda > 250$ nm irradiation.

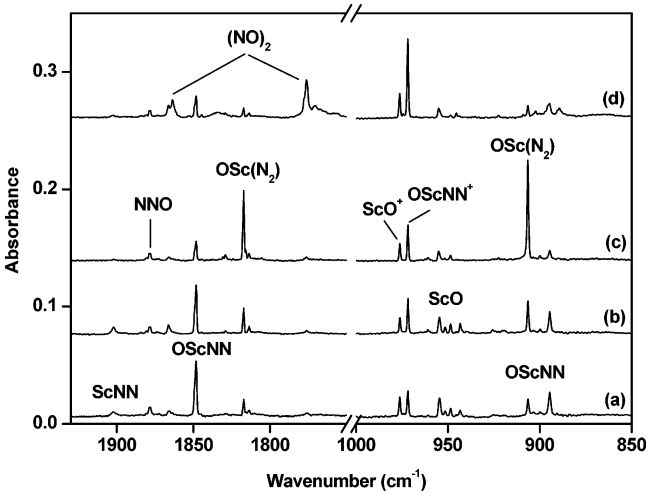

Figure 4. Infrared spectra in the 1930−1750 and 1000−850 cm^{-1} regions from codeposition of laser-evaporated Sc atoms with 0.2% N_2O in argon at 12 K. (a) 1 h of sample deposition, (b) after 25 K annealing, (c) after 20 min of $\lambda > 500$ nm irradiation, and (d) after 20 min of $\lambda > 250$ nm irradiation.

absorptions. The 1817.2 and 906.5 cm^{-1} bands were destroyed under subsequent broadband irradiation at the wavelength range of $250 < \lambda < 580$ nm (trace d), during which the absorptions at 2341.7 and 971.8 cm^{-1} greatly increased.

Calculation Results. Quantum chemical calculations were performed on the potential product molecules. The optimized structures are shown in Figure 5. The total energies, vibrational frequencies, and intensities of various species involved in the ScO/N_2 system are listed in Table 2.

Discussions

OSc(N_2). The absorptions at 1817.2 and 906.5 cm^{-1} were formed on annealing in the Sc_2O_3 + N_2/Ar experiments. These bands were also observed in the Sc + N_2O/Ar experiment but only under irradiation at the wavelength range of $400 < \lambda < 580$ nm. The 906.5 cm^{-1} band is in the spectral range expected for the terminal Sc−O stretching mode of a ScO complex. The 1817.2 cm^{-1} band shifted to 1756.6 cm^{-1} with the $^{15}N_2$/Ar sample. The $^{14}N/^{15}N$ isotopic frequency ratio of 1.0345 is indicative of a N−N stretching vibration. In the experiment with

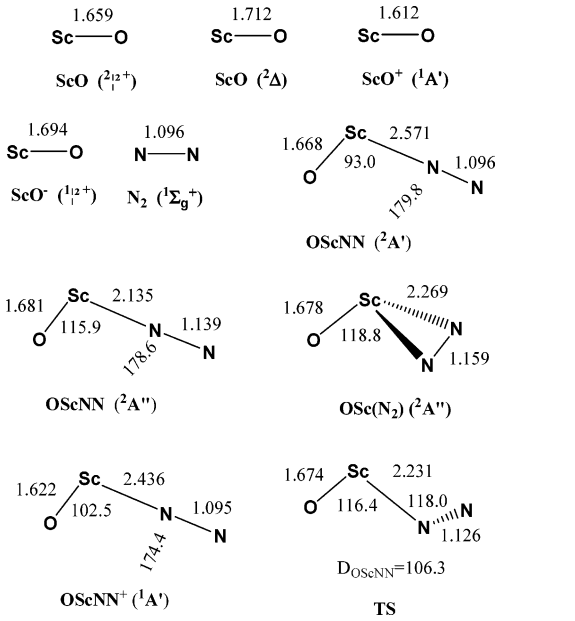

Figure 5. Optimized structures (bond lengths in Å and bond angles in deg) of various species involved in the ScO + N_2 reaction.

TABLE 2: Calculated Total Energies (in hartrees, after Zero Point Energy Correction), N−N and Sc−O Stretching Vibrational Frequencies (cm^{-1}), and Intensities (km/mol) of Various Species in the ScO/N_2 System

	energy	N−N str	Sc−O str
ScO ($^2\Sigma^+$)	−835.962972		999.8 (211)
ScO ($^2\Delta$)	−835.911406		879.1 (173)
ScO^+ ($^1\Sigma^+$)	−835.721323		1074.2 (170)
ScO^- ($^1\Sigma^+$)	−836.009338		934.1 (211)
N_2 ($^1\Sigma_g^+$)	−109.554125	2444.9 (0)	
OScNN (^{2}A′)	−945.518118	2408.5 (206)	976.5 (242)
OScNN (^{2}A")	−945.514212	1998.0 (898)	944.3 (433)
OSc(N_2) (^{2}A")	−945.519345	1939.1 (338)	958.2 (344)
$OScNN^+$ (^{1}A′)	−945.297792	2454.7 (28)	1058.9 (172)
TS	−945.507863		

a $^{14}N_2$ + $^{15}N_2$/Ar sample (Figure 2), only the 1817.2 and 1756.6 cm^{-1} bands were observed, indicating that only one N_2 is involved in the molecule. A triplet at 1817.2, 1787.0, and 1756.6 cm^{-1} with approximately 1:2:1 relative intensities was produced when a $^{14}N_2$ + $^{14}N^{15}N$ + $^{15}N_2$/Ar sample was employed (Figure 3). The above-mentioned spectral features imply that the two nitrogen atoms are equivalent. Accordingly, we assign the 906.5 and 1817.2 cm^{-1} bands to the Sc−O and N−N stretching vibrations of a side-bonded OSc(N_2) complex. The 1813.6 and 899.8 cm^{-1} bands observed in the Sc_2O_3 + N_2/Ar experiments showed the same isotopic shifts and splittings as the 1817.2 and 906.5 cm^{-1} bands. These bands could be assigned either to the OSc(N_2) complex at different matrix trapping site or to the OSc(N_2)$(NN)_x$ complex. Note that the 1813.6/899.8 cm^{-1} bands were not produced in the Sc + N_2O/Ar experiment, and that the 1813.6/899.8 cm^{-1} pair is favored upon annealing, whereas the 1817.2/906.5 cm^{-1} pair is favored upon irradiation, which suggest that the 1813.6/899.8 cm^{-1} bands are more likely due to the OSc(N_2)(NN)x complex.

Density functional calculations were performed to support the assignment. As shown in Figure 5, the side-bonded OSc(N_2) complex was predicted to have a ^{2}A″ ground state with a C_s symmetry, in agreement with the result recently calculated by Hwang and Mebel at the B3LYP/6-31G* level of theory.[13] The N−N and Sc−O stretching modes were computed at 1939.1 and 958.2 cm^{-1}. These two modes were computed to have the largest IR intensities. The Sc−O stretching mode was predicted

to be red-shifted by about 41.6 cm^{-1} with respect to the frequency of diatomic ScO calculated at the same level of theory, slightly smaller than the experimentally observed shift of 48.3 cm^{-1}. As will be reported,[31] the $OSc(N_2)$ complex can form complex with noble gas atoms in solid noble gas matrices. The Sc−O stretching frequency of $OSc(N_2)$ red-shifted additional 6.8 cm^{-1} when coordinated by two Ar atoms. Since the diatomic ScO molecule cannot form strong complex with argon,[32] the predicted Sc−O stretching frequency shift of ScO by coordination with N_2 and Ar ($41.6 + 6.8 = 48.4$ cm^{-1}) is in excellent agreement with the observed value of 48.3 cm^{-1}.

OScNN. The present experiments provide evidence for another scandium monoxide−dinitrogen complex with the stoichiometry of 1:1. In the $Sc_2O_3 + N_2$/Ar experiments, the initially formed $OSc(N_2)$ complex was destroyed by broadband irradiation, giving rise to the bands at 1849.2 and 894.6 cm^{-1}. These bands were also formed in the Sc + N_2O/Ar experiment, and were destroyed under $400 < \lambda < 580$ nm irradiation with the production of $OSc(N_2)$. The 1849.2 cm^{-1} band shifted to 1788.0 cm^{-1} with $^{15}N_2$/Ar. The $^{14}N/^{15}N$ isotopic ratio of 1.0342 also indicates a N−N stretching vibration. As shown in Figures 2 and 3, no intermediate absorption was observed in the $^{14}N_2 + {}^{15}N_2$/Ar spectra, while a 1:1:1:1 quartet with two intermediate absorptions at 1819.3 and 1817.8 cm^{-1} was seen in the $^{14}N_2 + {}^{14}N^{15}N + {}^{15}N_2$/Ar spectra. These mixed isotopic spectral features imply that the complex involves a N_2 subunit with two slightly inequivalent N atoms. The 894.6 cm^{-1} exhibited no shift with $^{15}N_2$ and is appropriate for the Sc−O stretching vibration of a ScO complex. Accordingly, we assign the 1849.2 and 894.6 cm^{-1} bands to the N−N and Sc−O stretching vibrations of an end-on bonded OScNN complex in solid argon matrix.

As shown in Figure 5, the ground state of the OScNN complex was predicted to be a $^2A'$ state, followed by a $^2A''$ state, which lies only about 10.5 kJ/mol above the $^2A'$ state. The $^2A'$ state correlates to the ground-state ScO ($^2\Sigma^+$) and N_2, and is very weakly bound with a Sc−N distance of 2.571 Å. The $^2A''$ state is derived from the $^2\Delta$ first excited state of ScO and N_2, and it is more strongly bound with a Sc−N distance of 2.135 Å. As listed in Table 2, the N−N and Sc−O stretching frequencies for the $^2A'$ state were computed at 2408.5 and 976.5 cm^{-1}. These vibrational frequencies are too large to match the experimentally observed frequencies. However, the frequencies of the $^2A''$ state calculated at 1998.0 and 944.3 cm^{-1} are in reasonable agreement with the experimental values. We suggest the possibility that the OScNN molecule exhibits a noble gas-induced ground-state reversal like that for CUO and UO_2.[33,34] Recent investigations on actinide compound in noble gas matrices have shown that actinide-containing molecules such as CUO and UO_2 can form strong complexes with the noble gas atoms. Noble gas-induced ground-state reversal was observed when two distinct electronic states are very close in energy.[33,34] As will be discussed,[31] the $^2A''$ state OScNN is coordinated by two Ar atoms in solid argon matrix. The calculation results indicate that the $^2A''$ state of OScNN can be sufficiently stabilized upon the coordination of two argon atoms to cause a noble gas-induced reversal of the ground state of the molecule. Therefore, the $^2A''$ state becomes the ground state in the presence of Ar atoms.

$OScNN^+$. The bands at 2341.7 and 971.8 cm^{-1} were mainly formed under broadband irradiation in the Sc + N_2O/Ar experiment. Because of the weak oscillator strength of the NN stretch, calculated to be six times weaker than the ScO stretch, the 2341.7 cm^{-1} band was not observed in the $Sc_2O_3 + N_2$/Ar experiments. The upper band is slightly higher than the N−N stretching frequency of N_2, while the lower mode is red-shifted by only 4.6 cm^{-1} from that of ScO^+. These bands are appropriate for the N−N and Sc−O stretching modes of the $OScNN^+$ complex. B3LYP calculations predicted the $OScNN^+$ to have a singlet ground state with planar C_s symmetry with N−N and Sc−O stretching frequencies at 2454.7 and 1058.9 cm^{-1}. Both ScO^+ and $OScNN^+$ form stable complexes with Ar atoms in solid argon.[31,32]

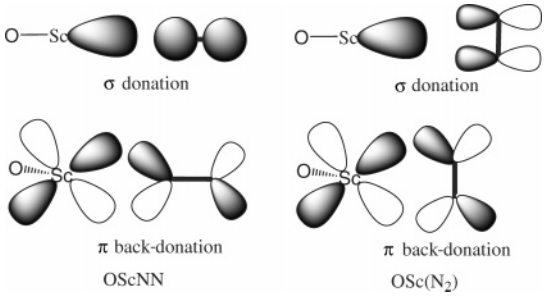

Figure 6. Principle orbital interactions in OScNN and $OSc(N_2)$.

Bonding Analysis. The well-studied ScO molecule has been shown to have a $^2\Sigma^+$ ground state with an electronic configuration of $...(8\sigma)^2(3\pi)^4(9\sigma)^1(1\delta)^0$. A $^2\Delta$ state with an electronic configuration of $...(8\sigma)^2(3\pi)^4(1\delta)^1(9\sigma)^0$ lies 170.1−180.6 kJ/mol higher in energy.[26,35] In our calculations, the $^2\Delta$ state lies 135.4 kJ/mol above the $^2\Sigma^+$ ground state. The 9σ molecular orbital is primarily a nonbonding hybrid of the Sc 4s and $3d_z^2$ orbitals that is directed away from the O atom. The 1δ molecular orbital is largely the Sc 3d orbital that is mainly nonbonding. The interactions between ScO and N_2 are dominated by the synergic donations of filled orbitals of N_2 into an empty acceptor orbital of ScO and the back-donation of the ScO electrons to the empty orbitals of N_2. Both the $^2A''$ state of $OSc(N_2)$ and OScNN complexes can be viewed as being formed by the interaction of the $^2\Delta$ first excite state of ScO fragment and the N_2 fragment. The principle orbital interactions in OScNN and $OSc(N_2)$ are shown in Figure 6. In both cases, the empty 9σ molecular orbital of ScO is the primary acceptor orbital for donation from the N_2 fragment. The filled $3\sigma_g$ molecular orbital of N_2 is the principal donor orbital in the end-on bonded OScNN complex; while the filled $1\pi_u$ molecular orbitals of N_2 are the principle donor orbitals in the side-bonded $OSc(N_2)$ complex. The singly occupied 1δ molecular orbital is the back-donation orbital. It can interact with the π_g antibonding orbitals of N_2 in either end-on or side-bonded geometry. As can be seen in Figure 6, the donation interactions favor a linear or planar geometry, whereas the back-donation interactions prefer geometry with the OSc bond perpendicular to the ScN_2 plane. The calculated structures of OScNN and $OSc(N_2)$ are the result of a compromise between the donation and back-donation interactions, with the back-donation being somewhat stronger than the donation interactions, and thus favoring a geometry with the OScN angle around 115°. Since the 9σ MO is singly occupied, and the 1δ MO is empty, the above-mentioned donation and back-donation interactions between the $^2\Sigma^+$ ground-state ScO and N_2 are much weaker than those of the $^2\Delta$ state ScO and N_2. Therefore, the ground state ScO can only form very weak complex with N_2. In contrast to the neutral OScNN and $OSc(N_2)$ complexes, the bonding interaction in the $OScNN^+$ cation complex is mainly electrostatic between the ScO^+ cation and N_2, which only favors an end-on bonded fashion.

Reaction Mechanism. In the $Sc_2O_3 + N_2$/Ar experiments, the ground-state ScO molecule reacted with N_2 to form the side-bonded $OSc(N_2)$ complex in solid argon, reaction 1. As has been discussed, the $OSc(N_2)$ complex correlates to the $^2\Delta$ first excite

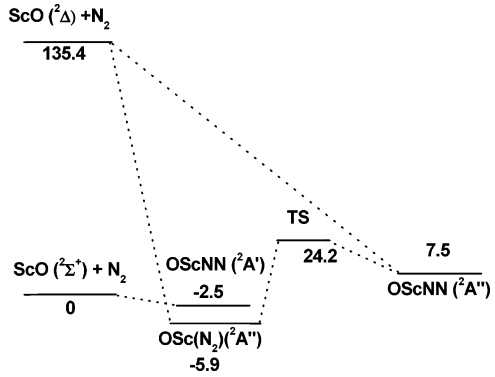

Figure 7. Potential energy profile of the ScO + N_2 reaction calculated at the B3LYP/6-311+G* level of theory. All relative energies are given in kJ/mol.

state of ScO. Formation of ^{2}A″ OSc(N_2) from the ground-state ScO involves crossing or avoided crossing of the ^{2}A′ and ^{2}A″ potential energy surface, as shown in Figure 7. The OSc(N_2) complex absorptions increased on annealing, indicating that this process requires no activation energy.

$$\mathrm{ScO}\ (^2\Sigma^+) + \mathrm{N_2} \rightarrow \mathrm{OSc(N_2)}\ (^2\mathrm{A}'')\ \Delta E = -5.9\ \mathrm{kJ/mol} \quad (1)$$

The OScNN absorptions markedly increased upon broadband ($250 < \lambda < 580$ nm) irradiation, during which the absorptions of the OSc(N_2) complex disappeared. This observation suggests that OSc(N_2) underwent photoinduced isomerism to OScNN, as shown in reaction 2. The isomerization reaction from OSc(N_2) (^{2}A″) to OScNN (^{2}A″) was predicted to be slightly endothermic (13.4 kJ/mol), and it proceeds via a transition state (Figure 7). This transition state lies 30.1 kJ/mol higher in energy than OSc(N_2) (^{2}A″).

$$\mathrm{OSc(N_2)}\ (^2\mathrm{A}'') + h\nu \rightarrow \mathrm{OScNN}\ (^2\mathrm{A}'') \quad (2)$$

In the Sc + N_2O/Ar experiment, the OScNN complex was observed after sample deposition. The OScNN complex must be formed by insertion reaction during the sample deposition process, reaction 3. The OScNN absorptions slightly decreased on annealing indicate that reaction 3 requires activation energy. The activation barrier for the ground-state Sc and N_2O reaction was determined to be 7.5 kJ/mol in previous gas-phase kinetic studies.[36,37] The OScNN absorptions decreased on $400 < \lambda < 580$ nm irradiation, while the amount of OSc(N_2) increased, which is consistent with the isomerization of OScNN to OSc(N_2), the reverse of reaction 2.

$$\mathrm{Sc} + \mathrm{N_2O} \rightarrow \mathrm{OScNN}\ (^2\mathrm{A}'') \quad (3)$$

The OScNN$^+$ cation complex was produced largely upon broadband ($250 < \lambda < 580$ nm) irradiation at the expense of the neutral complexes. This suggests that the OScNN$^+$ cation complex was formed by photoionization of the neutral complexes. Since the calculated ionization energy of OScNN (5.9 eV) exceeds the mercury arc energy (5.0 eV at 250 nm), it is probable that an OSc(N_2)* excited state, which can relax to the OSc(N_2) isomer, is sufficiently long-lived to absorb a second photon to reach ionization. The NNO_2^- anion absorptions also increased on broadband irradiation, and serves as a counterion to preserve the matrix electric neutral.

Conclusions

Scandium monoxide dinitrogen complexes: OSc(N_2), OScNN, and OScNN$^+$ have been prepared by the reactions of laser-evaporated scandium monoxide with N_2 or scandium atoms with N_2O in solid argon. The ground-state scandium monoxide molecule reacted with N_2 to form the side-bonded OSc(N_2) complex spontaneously on annealing. This complex rearranged to the end-on bonded OScNN complex upon UV irradiation. Laser-evaporated Sc atoms reacted with N_2O to give the insertion product, OScNN, which rearranged to the side-bonded OSc(N_2) complex upon $400 < \lambda < 580$ nm irradiation. The neutral complexes can also be photoionized to the OScNN$^+$ cation complex upon UV irradiation. Both the OSc(N_2) and OScNN complexes in solid argon can be assigned to have ^{2}A″ electronic state with C_s symmetry arising from the $^2\Delta$ first excited-state ScO.

Acknowledgment. We greatly acknowledge financial support from NNSFC (20125311) and the NKBRSF (2004-CB719501) of China.

References and Notes

(1) Burdett, J. K.; Turner, J. J. *Chem. Commun.* **1971**, 885. Klatzbucher, W.; Ozin, G. A. *J. Am. Chem. Soc.* **1975**, *97*, 2672.

(2) Chertihin, G. V.; Andrews, L.; Neurock, M. *J. Phys. Chem.* **1996**, *100*, 14609. Andrews, L.; Bare, W. D, Chertihin, G. V. *J. Phys. Chem. A* **1997**, *101*, 8417. Andrews, L.; Citra, A.; Chertihin, G. V.; Bare, W. D.; Neurock, M. *J. Phys. Chem. A* **1998**, *102*, 2561.

(3) Elustondo, F.; Mascetti, J. *J. Phys. Chem. A* **2000**, *104*, 3572.

(4) Beyer, M.; Berg, C.; Albert, G.; Achatz, U.; Joos, S.; Niedner-Schatteburg, G.; Bondybey, V. E. *J. Am. Chem. Soc.* **1997**, *119*, 1466.

(5) Lessen, D. E.; Asher, R. L.; Brucat, P. J. *Chem. Phys. Lett.* **1991**, *177*, 380. Asher, R. L.; Bellert, D.; Buthelezi, T.; Brucat, P. J. *J. Phys. Chem.* **1995**, *99*, 1068.

(6) Schwarz, J.; Heinemann, C.; Schwarz, H. *J. Phys. Chem.* **1995**, *99*, 11405. Heinemann, C.; Schwarz, J.; Schwarz, H. *J. Phys. Chem.* **1996**, *100*, 6088.

(7) Khan, F. A.; Steele, D. L.; Armentrout, P. B. *J. Phys. Chem.* **1995**, *99*, 7819.

(8) Bauschlicher, C. W., Jr.; Pettersson, L. G. M.; Siegbahn, P. E. M. *J. Chem. Phys.* **1987**, *87*, 2129. Bauschlicher, C. W., Jr.; Partridge, H.; Langhoff, S. R. *J. Phys. Chem.* **1992**, *96*, 2475.

(9) McKee, M. L.; Worley, S. D. *J. Phys. Chem. A* **1997**, *101*, 5600.

(10) Hidai, M.; Mizobe, Y. *Chem. Rev.* **1995**, *95*, 1115. Hidai, M. *Coord. Chem. Rev.* **1999**, *185*−*186*, 99.

(11) Richards, R. L. *Coord. Chem. Rev.* **1996**, *154*, 83.

(12) Siegbahn, P. E. M.; Blomberg, M. R. A. *Chem. Rev.* **2000**, *100*, 421.

(13) Hwang, D. Y.; Mebel, A. M. *Chem. Phys. Lett.* **2003**, *375*, 17.

(14) Chen, M. H.; Zhou, M. F.; Zhang, L. N.; Qin, Q. Z. *J. Phys. Chem. A* **2000**, *104*, 8627.

(15) Zhou, M. F.; Zhang, L. N.; Qin, Q. Z. *J. Phys. Chem. A* **2001**, *105*, 6407.

(16) Chen, M. H.; Wang, G. J.; Jiang, G. Y.; Zhou, M. F. *J. Phys. Chem. A* **2005**, *109*, 415.

(17) Chen, M. H.; Wang, X. F.; Zhang, L. N.; Yu, M.; Qin, Q. Z. *Chem. Phys.* **1999**, *242*, 81.

(18) Gaussian 03, Revision B.05, Frisch, M. J.; Trucks, G. W.; Schlegel, H. B.; Scuseria, G. E.; Robb, M. A.; Cheeseman, J. R.; Montgomery, J. A., Jr.; Vreven, T.; Kudin, K. N.; Burant, J. C.; Millam, J. M.; Iyengar, S. S.; Tomasi, J.; Barone, V.; Mennucci, B.; Cossi, M.; Scalmani, G.; Rega, N.; Petersson, G. A.; Nakatsuji, H.; Hada, M.; Ehara, M.; Toyota, K.; Fukuda, R.; Hasegawa, J.; Ishida, M.; Nakajima, T.; Honda, Y.; Kitao, O.; Nakai, H.; Klene, M.; Li, X.; Knox, J. E.; Hratchian, H. P.; Cross, J. B.; Adamo, C.; Jaramillo, J.; Gomperts, R.; Stratmann, R. E.; Yazyev, O.; Austin, A. J.; Cammi, R.; Pomelli, C.; Ochterski, J. W.; Ayala, P. Y.; Morokuma, K.; Voth, G. A.; Salvador, P.; Dannenberg, J. J.; Zakrzewski, V. G.; Dapprich, S.; Daniels, A. D.; Strain, M. C.; Farkas, O.; Malick, D. K.; Rabuck, A. D.; Raghavachari, K.; Foresman, J. B.; Ortiz, J. V.; Cui, Q.; Baboul, A. G.; Clifford, S.; Cioslowski, J.; Stefanov, B. B.; Liu, G.; Liashenko, A.; Piskorz, P.; Komaromi, I.; Martin, R. L.; Fox, D. J.; Keith, T.; Al-Laham, M. A.; Peng, C. Y.; Nanayakkara, A.; Challacombe, M.; Gill, P. M. W.; Johnson, B.; Chen, W.; Wong, M. W.; Gonzalez, C.; Pople, J. A. Gaussian, Inc.: Pittsburgh, PA, 2003.

(19) Becke, A. D. *J. Chem. Phys.* **1993**, *98*, 5648.

(20) Lee, C.; Yang, E.; Parr, R. G. *Phys. Rev. B* **1988**, *37*, 785.

(21) McLean, A. D.; Chandler, G. S. *J. Chem. Phys.* **1980**, *72*, 5639.

(22) Krishnan, R.; Binkley, J. S.; Seeger, R.; Pople, J. A. *J. Chem. Phys.***1980**, *72*, 650.

(23) Head-Gordon, M.; Pople, J. A.; Frisch, M. *Chem. Phys. Lett.* **1988**, *153*, 503.
(24) Chertihin, G. V.; Andrews, L.; Rosi, M.; Bauschlicher, C. W., Jr. *J. Phys. Chem. A* **1997**, *101*, 9085.
(25) Bauschlicher, C. W., Jr.; Zhou, M. F.; Andrews, L.; Johnson, J. R. T.; Panas, I.; Snis, A.; Roos, B. O. *J. Phys. Chem. A* **1999**, *103*, 5463.
(26) Wu, H. B.; Wang, L. S. *J. Phys. Chem. A* **1998**, *102*, 9129.
(27) Chertihin, G. V.; Andrews, L.; Bauschlicher, C. W., Jr. *J. Am. Chem. Soc.* **1998**, *120*, 3205.
(28) Kauffman, J. W.; Hauge, R. H.; Margrave, J. L. *J. Phys. Chem.* **1985**, *89*, 3541.
(29) Zhang, L. N.; Dong, J.; Zhou, M. F. *J. Phys. Chem. A* **2000**, *104*, 8882.
(30) Milligan, D. E.; Jacox, M. E. *J. Chem. Phys.* **1971**, *55*, 3404. Hacaloglu, J.; Suzer, S.; Andrews, L. *J. Phys. Chem.* **1988**, *88*, 5383.
(31) Zhou, M. F.; Xi, J.; Wang, G. J. To be published.
(32) Zhao, Y. Y.; Chen, M. H.; Zhou, M. F.; Andrews, L. To be published.
(33) Li, J.; Bursten, B. E.; Liang, B. Y.; Andrews, L. *Science* **2002**, *295*, 2242. Liang, B. Y.; Andrews, L.; Li, J. Bursten, B. E. *J. Am. Chem. Soc.* **2002**, *124*, 9016. Andrews, L.; Liang, B. Y.; Li, J.; Bursten, B. E. *J. Am. Chem. Soc.* **2003**, *125*, 3126.
(34) Li, J.; Bursten, B. E.; Andrews, L.; Marsden, C. J. *J. Am. Chem. Soc.* **2004**, *126*, 3424.
(35) Huber, K. P.; Herzberg, G. *Molecular Spectra and Molecular Structure IV: Constants of Diatomic Molecules*; Van Nostrand Reinhold: New York, **1979.**
(36) Ritter, D.; Weisshaar, J. C. *J. Phys. Chem.* **1990**, *94*, 4907.
(37) Futerko, P. M.; Fontijn, A. *J. Chem. Phys.* **1991**, *95*, 8065.